Methods in Ecology and Evolution

British Ecological Society

Methods in Ecology and Evolution 2015, **6,** 1026–1033 doi: 10.1111/2041-210X.12390

A new permutation technique to explore and control for spatial autocorrelation

Reinder Radersma[1,2]* and Ben C. Sheldon[1]

[1]*Department of Zoology, Edward Grey Institute, University of Oxford, Oxford OX1 3PS, UK; and* [2]*Department of Biology, Lund University, 22100 Lund, Sweden*

Summary

1. Permutation tests are important in ecology and evolution as they enable robust analysis of small sample sizes and control for various forms of dependencies among observations. A common source of dependence is spatial autocorrelation. Accounting for spatial autocorrelation is often crucial, because many ecological and evolutionary processes are spatially restricted, such as gene flow, dispersal, mate choice, inter- and intraspecific competition, mutualism and predation.

2. Here we discuss various ways of controlling for spatial autocorrelation in permutation tests; we highlight their particular properties and assumptions and introduce a new permutation technique which explores and controls for spatial autocorrelation: the floating grid permutation technique (FGPT).

3. The FGPT is a method to randomize observations with known geographical locations. Within the randomization process, the probability an observation is assigned to any of the spatial locations is a negative function of the distance between its original and assigned location. The slope of this function depends on a preset parameter, and by exploring its parameter space, non-random ecological and evolutionary processes can be both assessed and controlled at multiple spatial scales.

4. We show that the FGPT has acceptable type-I-error rates. We applied the FGPT to simulated univariate and bivariate data sets in which both negative and positive spatial autocorrelation were present. In comparison with a method that uses eigenvector decomposition to separate negative from positive spatial autocorrelation, the FGPT performed better for negative spatial autocorrelation alone, equal for positive spatial autocorrelation alone and equal or slightly worse for simultaneous negative and positive spatial autocorrelation. For the bivariate data, it performed equally to a bootstrapping technique in which sampling probabilities were weighted by distance. The FGPT benefits from a large flexibility for application to bivariate (e.g. dyadic interactions) and multivariate observations (e.g. genetic marker-based relatedness measures) and has a large freedom in the choice of test statistic. It also has the potential to identify two spatial autocorrelation patterns, even if both result in positive spatial autocorrelation, given that they operate at different spatial scales.

5. The Floating Grid Permutation Technique is available as the R-package *fgpt* in CRAN.

Key-words: bootstrap, point pattern, population stratification, randomization, R-package, SNPs, spatial autocorrelation, spatial distribution, spatially restricted

Introduction

Permutation or randomization tests have found increasing use in ecological and evolutionary studies as they tend to rely on fewer assumptions and are generally more flexible than parametric tests. For instance, while parametric tests assume that observations come from pre-specified theoretical frequency distributions, permutation tests use empirically derived distributions (Fortin & Jacquez 2000; Manly 2006). In particular with relative small sample sizes, which are quite common in ecology and evolution, the observed frequency distributions often mismatch theoretical distributions and therefore permutation tests offer a good alternative to parametric tests (Fortin & Jacquez 2000; Ruxton & Neuhäuser 2013). Permutation tests can also be tailored to test specific null models, for instance by using null models that do not assume complete randomness, but take some specific structures of the data into account (Manly 2006). This is particularly interesting for ecological and evolutionary data, because those types of observations are often not completely independent (Fortin & Jacquez 2000). For instance, many populations show genetic structure and experience variable environmental conditions. It must be noted that the generality of results from permutation tests has been disputed (which is at least to a lesser extent also the case for parametric tests; Fortin & Jacquez 2000; Legendre & Legendre 2012, pp. 25–32) and the flexibility for designing null models comes with the risk of designing inappropriate null models for the raised hypotheses.

An important and common form of dependence in ecological and evolutionary observations is spatial autocorrelation.

*Correspondence author. E-mail: reinder@rndr.nl

The spatial distributions of geno- and phenotypes are typically not random, as they are shaped by processes which are spatially restricted. For instance, external factors that are spatially structured (e.g. temperature, soil pH, vegetation structure and presence of prey items) cause local adaptation by natural selection or differential dispersal and therefore spatial heterogeneity in geno- and phenotypes (Fortin & Dale 2005; Legendre & Legendre 2012, pp. 11–12). On top of that endogenous biotic processes, such as genetic drift, limited dispersal, kin structure and population history may increase or cause additional spatial variation (Sokal & Oden 1978; Fortin & Dale 2005; Legendre & Legendre 2012, pp. 11–12).

In this paper, we focus on exploring and controlling for spatial autocorrelation in permutation tests. Permutation tests follow a five-step procedure. (i) First, a relevant question is determined which leads to a null hypothesis and one, or several, alternative hypotheses. (ii) Next, a statistic should be chosen or designed which is suitable for testing the hypotheses. (iii) This statistic is calculated for the observed data, and (iv) a null reference frequency distribution for this statistic is produced. The latter step involves randomizing the observed data many times (≥10 000 times) and calculating the statistic for those randomized data sets. By choosing a particular way of randomizing the data, which we will discuss in more detail, spatial autocorrelation can be taken into account. (v) Finally, the observed statistic is compared to the null reference frequency distribution for this statistic and should lead to a decision to reject the null hypothesis or not (Fortin & Jacquez 2000; Manly 2006; Ruxton & Neuhäuser 2013).

There are many methods to explore or control for the non-random distribution of genotypes or phenotypes in space within the randomization process. Here we present a short non-comprehensive overview of some of the methods used. We start with randomization techniques that are spatially restricted (i.e. stratified sampling techniques), and next, we discuss other randomization techniques. Testing the randomness of the spatial distribution of the observations itself, or correlations between the spatial distribution and observations at those locations (i.e. marks), is beyond the scope of this paper; we refer the interested reader to, for instance, Cox & Isham (1980), Penttinen, Stoyan & Henttonen (1992), Diggle (2003) or Møller & Waagepetersen (2004).

One method to spatially restrict randomization is by restricted permutation within geographical regions. This null model assumes that the observations are randomly distributed over the sampling locations within those regions, but non-random between regions. This technique is particularly suitable when observations are clustered in distinct entities or patches (Fortin & Jacquez 2000). Examples of this method can be found in studies on intersexual selection (e.g. Van de Casteele & Matthysen 2006; Kasumovic *et al.* 2008). Randomizations could also be restricted among neighbouring sampling locations. This method makes use of bootstrapping rather than shuffling, because the same observations can be sampled more than once in any iteration and depends on some quantification of what neighbouring sites are. This technique has been used for studying inbreeding avoidance (e.g. Keller & Arcese 1998; Szulkin *et al.* 2009). Rather than using a discrete cut-off between neighbouring locations (which are sampled) and non-neighbours (which are not sampled), one could also use weighted sampling probabilities that are a function of the distance between each geographical location and the location for which a sample is drawn. Again, this method does not allow for shuffling, but relies on bootstrapping.

Other techniques include toroidal shift and using modelling techniques. In the toroidal shift, the spatial structure is maintained as it is and a layer with one type of observations randomly moved over another layer. The random movements can be restricted in one or more directions to maintain certain spatial patterns. This technique does not work for point pattern data with irregular sampling locations, but works for lattice data. This method assumes that spatial patterns are repeated outside the research area (Fortin & Jacquez 2000).

Lastly, one could also use one of the many spatial modelling techniques available to predict values for all observations. These predictions could be either used as null distribution (Fortin & Jacquez 2000) or the residuals could be randomized. Discussing the different ways to model spatial patterns is beyond the scope of this paper, and we would like to refer to chapter 7 of Borcard, Gillet & Legendre (2011) and chapter 13 of Legendre & Legendre (2012) for extensive explanations of methods for spatial analysis and their practical application. A combination of this method with the floating grid permutation technique, which is introduced here, will be touched upon in the discussion.

Here we introduce the floating grid permutation technique for performing spatially restricted permutation tests. The floating grid permutation technique sets apart different ecological or evolutionary mechanisms when they operate at different spatial scales and quantifies the spatial scales at which those mechanisms operate. We illustrate this method with some examples. The floating grid permutation technique is available as the R-package *fgpt* in the Comprehensive R Archive Network (CRAN; http://cran.r-project.org/web/packages/fgpt/). The R-package contains both lower level functions, to produce for instance randomized data sets, and higher level functions to perform complete analyses, and to produce plots and summary tables. A vignette is available on CRAN to further introduce the use of the R-package.

Methods

FLOATING GRID PERMUTATION TECHNIQUE

The Floating Grid Permutation Technique is a stratified sampling technique which results in a correlation between the distance between two sampling points and the probability that the observation at one of those locations will be assigned to the other location within the randomization procedure.

In the Floating Grid Permutation Technique, a set of grid cell sizes is chosen, which represents the different spatial scales that will be examined. The null distribution of observations for a particular grid cell size is calculated by first projecting the grid on a map of the geographical locations (Fig. 1a). Next, the grid is randomly moved and rotated

(Fig. 1b). Within each grid cell, observations are shuffled or, when appropriate, sampled with replacement (bootstrapped). The statistic appropriate for testing the hypotheses is calculated. The procedure is repeated a large number of times (≥10 000; Manly 2006) to produce a reference null distribution of the statistic (Fig. 1c). The probability of an observation being shuffled to any given location is a negative near-linear function of distance between the original and the given location (Fig. 1d; Supporting information). *P*-values can be calculated for all grid cell sizes and compared to a significance level. The null hypotheses for all grid cell sizes each assume biological processes (such as dispersal) to result in a random spatial distribution of observations within a particular spatial distance. The algorithm for this permutation technique can be found in Appendix S1.

APPLICATION OF THE FLOATING GRID PERMUTATION TECHNIQUE

We present some simulations to illustrate the FGPT. We first test the FGPT with simulations of univariate data and next illustrate the flexibility of the method with a bivariate example. Four additional multivariate examples of the application of the FGPT can be found in the supplementary materials, in each case motivated by a specific biological example. These are, respectively, (i) detecting inbreeding avoidance in a population with kin structure, (ii) separating the effect of habitat assortment and size-assortative pairing in an invertebrate, (iii) detecting self-pollination in a plant with variable mating system and (iv) detecting habitat selection in a foraging mammal in a patchy environment.

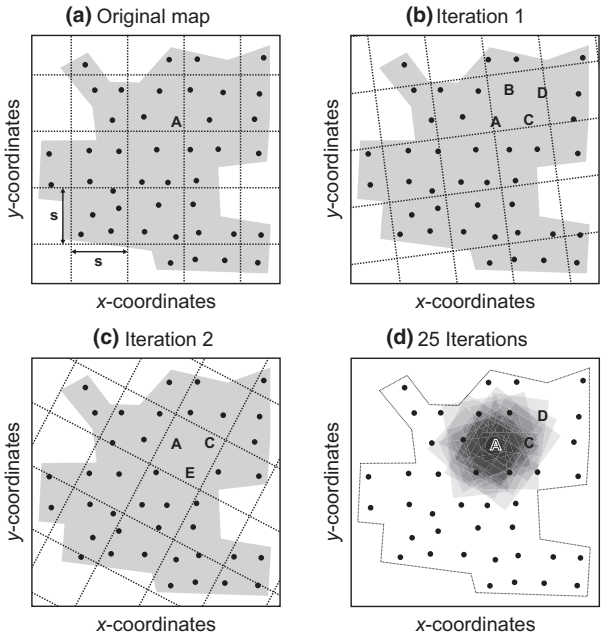

Fig. 1. A graphical representation of the floating grid permutation technique. The grey areas represent the study area, and black dots and capital letters represent locations of observations. (a) A grid of size *s* is projected on the original map of the area with our focal observation marked as A. (b) At the first iteration, the grid is randomly moved and rotated. Observations B, C and D share the same grid cell with A. Within each grid cell, all observations are randomized. (c) At the next iteration, A shares a grid cell with only two other observations, C and E. Again, all observations are randomized within grid cells, so A is randomized with C and E. (d) After many iterations (for graphical purposes, we show only 25), we get a empirical frequency distribution for the probability an observation is assigned to any of the spatial locations. The probability that A is assigned to the location of observation C is higher than to the location of observation D. This method assumes probability of being assigned to a specific location decreases with distance to the observed location.

Geographical locations

For the univariate examples, we simulated 100, 225 and 400 observations for both randomly spaced geographical locations and locations spaced on regular grids. For the bivariate example, we simulated 100 randomly spaced geographical locations. We drew the (*x* and *y*) coordinates for the random geographical locations independently from a uniform frequency distribution from 0 to 1. Regular geographical locations were placed on a squared (10-by-10, 15-by-15 or 20-by-20) lattice. For simulating spatial autocorrelated observations and some of the analyses (as explained below), spatial weighting matrices were necessary. Spatial weighting matrices model the assumed strength of the interactions between observations. Depending on the number of observations, we constructed a 100-by-100, 225-by-225 or 400-by-400 symmetric spatial weighting matrix in which both rows and columns correspond to the observations and with values of 1 s for neighbouring locations and 0 s for all other combinations. In case of random spacing, neighbouring locations were defined as locations which were closer than or as close as the longest edge of the minimum spanning tree (i.e. the minimum distance required to produce a completely connected network of geographical locations). In case of regular spacing, neighbouring locations were defined as locations which were directly next to or diagonally next to each other, which is the so-called queen neighbour definition (i.e. all locations within or at a distance of $\sqrt{2}$ times the cell size).

Univariate simulations

To illustrate the use of the FGPT for testing negative and positive spatial autocorrelation simultaneously, we produced sets of univariate observations with varying degrees of negative and positive spatial autocorrelation. We used 16 combinations of negative and positive spatial autocorrelation which were produced with four negative autoregressive parameters (ρ^-: 0, −0·3, −0·6 and −0·9) and four positive autoregressive parameters (ρ^+: 0, 0·3, 0·6 and 0·9). For all 16 combinations of ρ^- and ρ^+ we produced 1000 spatial autocorrelation patterns by summing the outcomes of two simultaneously autoregressive (SAR) models; one for the negative and one for the positive autoregressive parameter. This model is described in more detail in Dray (2011) and can be written as:

$$x = (I - \rho^- W)^{-1} y_1 + (I - \rho^+ W)^{-1} y_2,$$

in which I is the identity matrix, W is the row-standardized spatial weighting matrix, and y_1 and y_2 are column vectors of random values drawn from a normal frequency distribution with a mean of 0 and a variance of 1. The statistic we used to test for spatial autocorrelation in univariate data was Moran's I. Moran's I is a measure of spatial autocorrelation and for which values smaller than $\frac{-1}{N-1}$ – in which N is the number of observations – indicate negative spatial autocorrelation and larger values indicate positive spatial autocorrelation (Moran 1950; Legendre & Legendre 2012, p. 793). We chose to perform the FGPT at 15 different spatial scales $\{\frac{1}{15}d_{\max}, \frac{2}{15}d_{\max}, \ldots, \frac{15}{15}d_{\max}\}$ in which $d_{\max}$ is the maximum distance between any of the observations. For each spatial scale, we produced 9999 permuted data sets which we used to calculate reference distributions for Moran's I and we added the Moran's I of the observed values to the reference distributions. We analysed each

spatial autocorrelation pattern at the 15 spatial scales first for negative spatial autocorrelation, by calculating *P*-values for the hypothesis that the observed Moran's I was smaller than the reference distributions using one-sided significance levels ($\alpha = 0{\cdot}05$). We confirmed negative spatial autocorrelation if at least one of the 15 spatial scales resulted in a *P*-value lower than the significance level. We repeated the procedure for positive spatial autocorrelation, by calculating *P*-values for the hypothesis that the observed Moran's I was larger than the reference distributions rather than smaller. We compared the results with the results of the eigenvector decomposition method presented in Dray (2011). This method splits the spatial weighting matrix into positive and negative eigenvectors, which are used to calculate Moran's I for both positive and negative spatial autocorrelation.

Bivariate simulations

To illustrate the flexibility of the FGPT using a different test statistic, we performed a simulation in which we analysed bivariate data. For each of 100 randomly spaced locations, we simulated two observations that correlated negatively which each other. We added positive spatial autocorrelation to these observations, which was produced with a 200×200 spatial weighting matrix, for which 200 was the total number of observations (so two times the number of spatial locations). The rows and columns of the spatial weighting matrix corresponded to the stacked column vectors containing the first and the second observations. Neighbouring locations were defined as locations which were closer than or as close as the longest edge of the minimum spanning tree. This resulted in paired observations being regarded as neighbours and sharing all their neighbours. Again, we used 16 combinations of negative correlation and positive spatial autocorrelation which were produced with four negative correlation parameters (ρ^-: 0, −0·3, −0·6 and −0·9) and four positive autoregressive parameters (ρ^+: 0, 0·3, 0·6 and 0·9). For all 16 combinations of ρ^- and ρ^+ we produced 1000 spatial autocorrelation patterns by using a SAR model. This model can be written as:

$$x = (I - \rho^+ W)^{-1}\mathrm{vec}(Y)$$

in which I is the identity matrix, W is the row-standardized spatial weighting matrix, and vec (Y) is the vectorization of Y, the 100×2 matrix in which the columns are the two sets of observations. Y was drawn from a bivariate normal frequency distribution,

$$Y \sim \mathrm{MVN}(0, \Omega)$$

with means of zero and the variance – covariance matrix Ω being defined as:

$$\Omega = \begin{bmatrix} 1 & \rho^- \\ \rho^- & 1 \end{bmatrix}$$

in which the variances are one, and therefore, the covariances equal the correlation between both observations, in this case ρ^-. We chose to perform the FGPT at 15 different spatial scales $\{\frac{1}{15}d_{\max}, \frac{2}{15}d_{\max}, \ldots, \frac{15}{15}d_{\max}\}$ in which $d_{\max}$ is the maximum distance between any of the observations. At each iteration, only the first set of observations was permuted, in which the second one was kept the same. As test statistic, we used the Pearson product-moment correlation coefficient. For each spatial scale, we produced 9999 permuted data sets that allowed for resampling within iterations. We added the observed values to the reference distributions. We compared the method to another method, in which for each location observations were drawn from the empirical frequency distribution in which the probabilities were weighted as a function of the distance between the original location and all other locations. To make the two methods as comparable as possible, we decided to produce a function which resembled the FGPT closely:

$$p_{ij}(d_{ij}) = \begin{cases} 1 - \frac{d_{ij}}{s}, & d_{ij} \leq s \\ 0, & d_{ij} > s \end{cases}$$

in which p_{ij} is the probability of the observation of location j being sampled for location i, d_{ij}, the distance between location i and j and s the grid cell size of the FGPT analysis to which the analysis is compared to. This function approaches the relationship produced by the FGPT (see Supporting information).

EDGE EFFECTS

The results of the Floating Grid Permutation Technique are potentially affected by the boundaries of the study area. High edge-to-area ratio increases variation in the number of observations per grid cell. To investigate those properties, we simulated additional edges in the 10-by-10 lattice described above. We simulated additional edges by making use of group memberships. We split the 10-by-10 grid into three or five areas to create, respectively, 50% and 100% of additional edges. The three areas consisted of 3-by-10, 4-by-10 and 3-by-10 observations; the five areas consisted all of 2-by-10 observations (Fig. 4). In this way, we kept the number of observations and the distances between observations the same and minimally affected the maximum possible distances between observations. For three sets of observations (without, with 50% and with 100% additional edges) we produced 1000 negative and 1000 positive spatial autocorrelation patterns with a SAR model,

$$x = (I - \rho W)^{-1} y$$

in which I is the identity matrix, ρ is either the negative or positive autoregressive parameter, W is the row-standardized spatial weighting matrix, and y is a column vector of random values drawn from a normal frequency distribution with a mean of 0 and a variance of 1. The negative and positive autoregressive parameters were sampled from uniform frequency distributions from −0·95 to 0 and 0 to 0·95, respectively. Edge effects are a common issue in spatial statistics (Fortin & Dale 2005, pp. 22–24), and it depends on the study system whether corrections for edge effects are needed. For instance, when the boundaries of the study area are also the physical boundaries of the occurrence of the study species, it is a property of the population rather than a methodological issue.

Results

UNIVARIATE SIMULATIONS

The results for the univariate example for 100, 225 and 400 observations can be found in Fig. 2, Figs S2 and S3, respectively. In all cases, the type-I-error rate of the FGPT (the probability of detection spatial autocorrelation, while there was none) was between 4·0 and 5·7% and did not differ significantly from the used threshold of 5% (exact binomial tests, $P \geq 0{\cdot}167$). We compared the results of the FGPT with the eigenvector method. We found that the FGPT was equally or more successful in detecting negative spatial autocorrelation, when there was no positive spatial autocorrelation, and equally successful in detecting positive spatial autocorrelation, when there was no negative spatial autocorrelation. The eigenvector

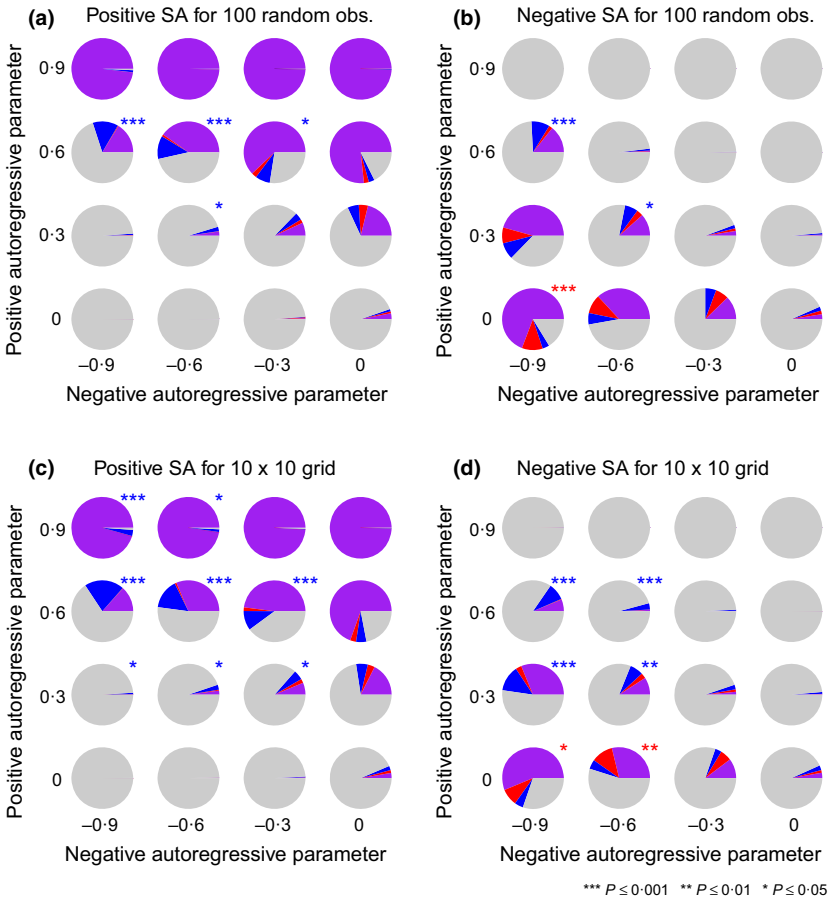

Fig. 2. Pie charts of the probabilities to detect (a,c) positive and (b,d) negative spatial autocorrelation for (a,b) 100 randomly or (c,d) regularly spaced univariate observations, given varying degrees of positive and negative spatial autocorrelation. Grey indicates positive or negative spatial autocorrelation not detected, red indicates only detected with the FGPT, blue indicates only detected with eigenvector decomposition, and purple indicates detected with both the FGPT and eigenvector decomposition.

method was equally or more successful in detecting positive spatial autocorrelation, when both were present (Fig. 2, Figs S2 and S3). Detection probabilities for both positive and negative spatial autocorrelations were higher for observations on random locations than on a grid. Detection probabilities were also higher with increasing numbers of observations.

BIVARIATE SIMULATIONS

The results for the bivariate example can be found in Fig. 3. The type-I-error rate of the FGPT was 3·8% and did not differ significantly from the used threshold of 5% (exact binomial test, $P = 0{\cdot}101$). We compared the results of the FGPT with the weighted bootstrapping technique in which sampling probabilities were a function of distance. The FGPT performed equally in detecting negative and positive spatial autocorrelation (Fig. 3).

EDGE EFFECTS

The additional edges resulted for negative spatial autocorrelation in small non-significant drops in the detection rate (150% edge: $\chi^2_1 = 0{\cdot}55$, $P = 0{\cdot}458$; 200% edge: $\chi^2_1 = 2{\cdot}39$, $P = 0{\cdot}122$; Fig. 4). For positive spatial autocorrelation, 150% edge resulted in a non-significant drop of detection rate ($\chi^2_1 = 0{\cdot}21$, $P = 0{\cdot}644$) and 200% edge in a slight significant drop of detection rate ($\chi^2_1 = 6{\cdot}19$, $P = 0{\cdot}013$; Fig. 4).

Discussion

In this paper, we showed how the FGPT can be used to disentangle various forms of spatial autocorrelation acting at different spatial scales; we for instance showed that negative and positive spatial autocorrelation can simultaneously be detected. The FGPT has a low type-I-error rate and has the ability to separate negative and positive spatial autocorrelation. The FGPT can also indicate the presence of at least two spatial processes even when they both result in positive spatial autocorrelation, given they act on different spatial scales (see Supporting information).

As a permutation test, the FGPT enjoys a great flexibility in the choice of test statistic, and on top of that, one can also choose the randomization protocol. The preferred test statistic depends on the data and the research question. Test statistics can be, but are not limited to the following: univariate statistics such as means and variances, bivariate statistics such as distances and correlations, multivariate statistics such as genetic distances or statistics derived from more complicated models with covariates or hierarchical data structures such as regressions and other ANOVAs. The preferred randomization protocol depends on the biological processes that are assumed under the null hypothesis. For instance, one can either shuffle in which all observations are sampled once in each iteration or bootstrap in which some observations will be sampled multiple times, while are not sampled at all in each iteration. Shuffling

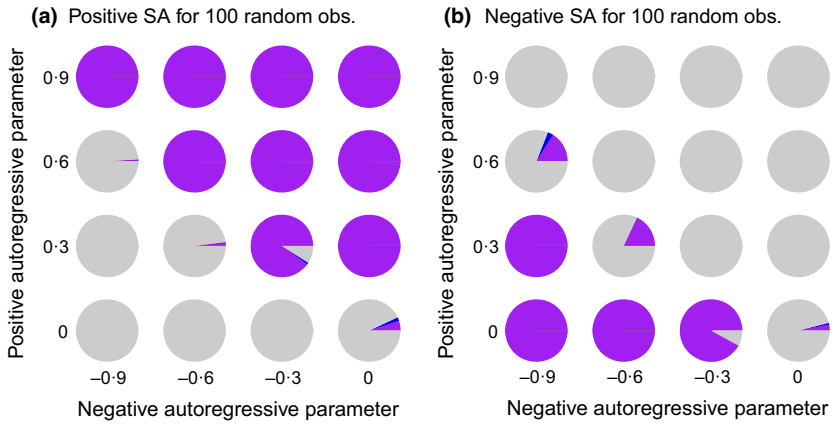

Fig. 3. Pie charts of the probabilities to detect (a) positive and (b) negative spatial autocorrelation for 100 randomly spaced paired bivariate observations, given varying degrees of positive and negative spatial autocorrelation. Grey indicates positive or negative spatial autocorrelation not detected, red indicates only detected with the FGPT, blue indicates only detected with eigenvector decomposition, and purple indicates detected with both the FGPT and eigenvector decomposition.

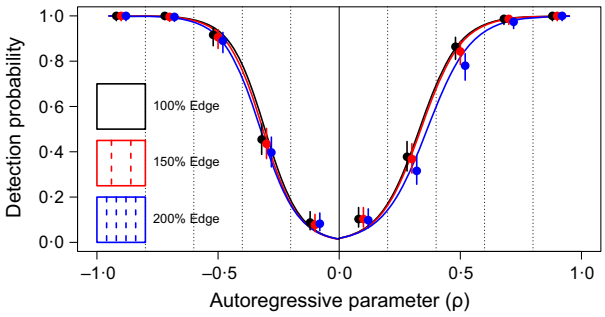

Fig. 4. Detection probabilities of spatial autocorrelation with the FGPT given additional edges. Black indicates without additional edges, red is with 50% extra edges, and blue is with 100% extra edges. Curves are fitted generalized linear models with a logit error distribution. Dots and error bars are means and Wilson's confidence intervals for binned probabilities, respectively.

assumes a biological process in which observations can only occur at one spatial location (e.g. individuals can only hold one territory), which bootstrapping assumes that observations can occurs at multiple spatial locations at the same time (e.g. an individual plant can pollinate multiple other plants). Many permutation tests, like the ones we described in the introduction and compared the FGPT to, are flexible in the choice of test statistic or the randomization protocol, but not both.

In the univariate simulations, we compared the FGPT to the eigenvector decomposition method introduced by Dray (2011). The eigenvector decomposition method was better able to detect spatial autocorrelation, particularly for positive spatial autocorrelation. The probability of detecting true positives with the FGPT improved for larger data sets. The eigenvector decomposition method is, however, limited to test for spatial autocorrelation in univariate data sets and only with Moran's I, while the FGPT is more flexible and can be used for other test statistics. In the bivariate simulations, we compared the FGPT to a permutation test in which the sampling probabilities depended on distance. The methods performed equally in detecting spatial autocorrelation in paired and correlated observations. The major benefit of the FGPT was its flexibility with respect to the randomization protocol, while the other method could only use bootstrapping.

In our simulation, the eigenvector decomposition method was less successful in detecting negative spatial autocorrelation than in Dray (2011). An important difference between both studies is the neighbour definition used for simulating data. Dray (2011) used observations on a lattice with rook configuration ($\leq$1 lattice cell size), while we used queen configuration ($\leq\sqrt{2}$ lattice cell size) for the lattice and the maximum distance of the minimum spanning tree for the randomly located observations. With the same negative autoregressive parameter (ρ^-), rook configuration results in much stronger negative spatial autocorrelation than queen or the maximum distance of the minimum spanning tree does (Fig. S4). This results in a discrepancy between the negative spatial autocorrelation produced with rook and queen configuration, while using the same autoregressive parameter. In our simulations of observations on a lattice, we chose to use queen configuration rather than rook configuration, because queen configuration is closer to a distance-based definition, which is assumed by the FGPT (Fig. S1).

An alternative method that can be used for analysing correlations between two sets of observations at different spatial scales is the multiscale codependence analysis (MCA; Guénard *et al.* 2010). MCA selects the strongest correlation between two sets of observations, while accounting for different sets of orthogonal spatial axes. MCA should be better able to find patterns caused by processes that vary in space, but is limited which respect to the test statistic that is used.

It is important to note that positive and negative spatial autocorrelation are definitions which depend on the spacing of observations as well as the size of the area of investigation. What is regarded as negative spatial autocorrelations at very large scales can be regarded as positive spatial autocorrelation at much smaller scales (Fortin & Dale 2005). This is also the case for the FGPT. With respect to scale, the FGPT has an interesting property which it does not share with methods based on eigenvector decomposition, such as Dray's method (Dray 2011) and MCA (Guénard *et al.* 2010). By default, the FGPT uses spatial scales based on the size of the study area, which is comparable to the eigenvector methods for which the spatial weighting matrix is shaped by spacing of the observations and the size of the area. But in the FGPT, the spatial scales can also be fixed at particular grid cell sizes, making

direct comparison of the scales of biological processes between differently sized study areas possible. For eigenvector methods, this is not possible because spatial weighting matrices are unique for each set of locations and do generally not translate linearly to spatial distances.

The FGPT uses rectangular grids. A common alternative would be the use of hexagonal grids, which are more balanced and closer approximations of round cells. Round cells would result in a perfect linear relationship between the distance between two locations and the probability the observation at one of those locations will be assigned to the other and are therefore preferential, but are perhaps a poor way to represent the way that organisms partition space as they either overlap or do not result in a complete filling of habitat. In the supplementary materials (Fig. S1), we show that squared and hexagonal grids do not differ quantitatively from each other with respect to the approximation of this linear relationship. For practical reasons, we therefore implemented rectangular grids in the Floating Grid Permutation Technique.

A way to further investigate spatial patterns in the data, which is not exclusively applicable to the FGPT, is the removal of spatial patterns before analyses. For instance, comparing patterns before and after the removal of large-scale spatial patterns can potentially lead to the discovery of fine-scale patterns, as illustrated by one of the examples in the supplementary materials. In one of the examples in the supplementary material, we used trend surface analysis that only accounts for linear or polynomial clines. However, more sophisticated methods to model and remove spatial autocorrelation like eigenvector-based methods (Borcard & Legendre 2002; Borcard *et al*. 2004; Griffith & Peres-Neto 2006) can be used as well. Note that eigenvector-based methods have the capacity to provide detailed models describing all spatial variation. Therefore, eigenvectors must be selected carefully to prevent the removal of patterns of interest. For instance, when using eigenvector-based methods to remove broad spatial patterns in order to focus on fine-scale patterns, only global eigenvector maps (describing broad patterns) should be used and no local eigenvector maps. See chapter 7 of Borcard, Gillet & Legendre (2011) and chapter 13 of Legendre & Legendre (2012) for extensive explanations of methods for spatial analysis and their practical application.

A particularly interesting feature of the floating grid permutation technique is that it can detect non-random mating in spatially structured populations. Recent studies have suggested that genetic structure can be present at very fine spatial scales well within the natal dispersal range of the species (e.g. Nichols *et al*. 2012; Garroway *et al*. 2013). If, in such cases, inbreeding avoidance is present, a non-spatial permutation test might not detect disassortative mating or even suggest the presence of assortative mating. The floating grid permutation technique, however, is able to detect inbreeding avoidance.

In summary, this study introduces a new spatially restricted permutation test. This method indicates at which spatial scales different spatial processes take place. The method is free of assumptions regarding the spatial scale those processes are expected. Therefore, it is very suitable for systems in which there is no extensive knowledge about the scale of biological processes and can be used in populations that show genotypic or phenotypic variation in space.

Acknowledgements

This study was funded by an ERC Advanced Investigator Award to BCS (AdG 250164). We thank Stéphane Dray, Gavin Simpson and the anonymous reviewers for their constructive comments on earlier drafts of this manuscript.

Data accessibility

R scripts for reproducing the examples are uploaded as online supporting information.

References

Borcard, D., Gillet, F. & Legendre, P. (2011) *Numerical ecology with R*. Springer Verlag, New York.

Borcard, D. & Legendre, P. (2002) All-scale spatial analysis of ecological data by means of principal coordinates of neighbour matrices. *Ecological Modelling*, **153**, 51–68.

Borcard, D., Legendre, P., Avois-Jacquet, C. & Tuomisto, H. (2004) Dissecting the spatial structure of ecological data at multiple scales. *Ecology*, **85**, 1826–1832.

Cox, D.R. & Isham, V. (1980) *Point processes*. Chapman & Hall/CRC, Boca Raton.

Diggle, P. (2003) *Spatial analysis of spatial point pattern*. Arnold, London.

Dray, S. (2011) A new perspective about Moran's coefficient: spatial autocorrelation as a linear regression problem. *Geographical Analysis*, **43**, 127–141.

Fortin, M.-J. & Dale, M. (2005) *Spatial Analysis: A Guide for Ecologists*. Cambridge University Press, Cambridge.

Fortin, M. & Jacquez, G. (2000) Randomization tests and spatially autocorrelated data. *Bulletin of the Ecological Society of America*, **81**, 201–205.

Garroway, C.J., Radersma, R., Sepil, I., Santure, A.W., De Cauwer, I., Slate, J. & Sheldon, B.C. (2013) Fine-scale genetic structure in a wild bird population: the role of limited dispersal and environmentally-based selection as causal factors. *Evolution*, **67**, 3488–3500.

Griffith, D. & Peres-Neto, P. (2006) Spatial modeling in ecology: the flexibility of eigenfunction spatial analyses. *Ecology*, **87**, 2603–2613.

Guénard, G., Legendre, P., Boisclair, D. & Bilodeau, M. (2010) Multiscale codependence analysis: an integrated approach to analyze relationships across scales. *Ecology*, **91**, 2952–2964.

Kasumovic, M.M., Bruce, M.J., Andrade, M.C.B. & Herberstein, M.E. (2008) Spatial and temporal demographic variation drives within-season fluctuations in sexual selection. *Evolution; International Journal of Organic Evolution*, **62**, 2316–2325.

Keller, L.F. & Arcese, P. (1998) No evidence for inbreeding avoidance in a natural population of song sparrows (*Melospiza melodia*). *The American naturalist*, **152**, 380–392.

Legendre, P. & Legendre, L. (2012) *Numerical ecology*, 3rd English edn. Elsevier, Amsterdam.

Manly, B.F.J. (2006) *Randomization, bootstrap and Monte Carlo methods in biology*. Chapman & Hall/CRC, Boca Raton.

Møller, J. & Waagepetersen, R.P. (2004) *Statistical inference and simulation for spatial point processes*. Chapman & Hall/CRC, Boca Raton.

Moran, P.A.P. (1950) Notes on continuous stochastic phenomena. *Biometrika*, **37**, 17–23.

Nichols, H.J., Jordan, N.R., Jamie, G.A., Cant, M.A. & Hoffman, J.I. (2012) Fine-scale spatiotemporal patterns of genetic variation reflect budding dispersal coupled with strong natal philopatry in a cooperatively breeding mammal. *Molecular ecology*, **21**, 5348–5362.

Penttinen, A., Stoyan, D. & Henttonen, H.M. (1992) Marked point processes in forest statistics. *Forest Science*, **38**, 806–824.

Ruxton, G.D. & Neuhäuser, M. (2013). Improving the reporting of P -values generated by randomization methods. *Methods in Ecology and Evolution* (ed. R.B. O'Hara), **4**, 1033–1036.

Sokal, R.R. & Oden, N.L. (1978) Spatial autocorrelation in biology. 1. Methodology. *Biological Journal of the Linnean Society*, **10**, 199–228.

Szulkin, M., Zelazowski, P., Nicholson, G. & Sheldon, B.C. (2009) Inbreeding avoidance under different null models of random mating in the great tit. *Journal of Animal Ecology*, **78**, 778–788.
Van de Casteele, T. & Matthysen, E. (2006) Natal dispersal and parental escorting predict relatedness between mates in a passerine bird. *Molecular ecology*, **15**, 2557–2565.

Received 26 January 2015; accepted 2 April 2015
Handling Editor: Stephane Dray

Supporting Information

Additional Supporting Information may be found in the online version of this article.

Fig. S1. The relationship between the distance between two observations and the probability those observations will share a grid cell.

Fig. S2. Pie charts of the probabilities to detect (a,c) positive and (b,d) negative spatial autocorrelation for (a,b) 225 randomly or (c,d) regularly space univaraite observations, given varying degrees of positive and negative spatial autocorrelation.

Fig. S3. Pie charts of the probabilities to detect (a,c) positive and (b,d) negative spatial autocorrelation for (a,b) 400 randomly or (c,d) regularly space univaraite observations, given varying degrees of positive and negative spatial autocorrelation.

Fig. S4. Density plots of Morans' I produced by SAR-models for (a,d,g) the negative spatial autocorrelation component, (b,e,h) the combined spatial autocorrelation component and (c,f,i) the positive spatial autocorrelation component for 5000 simulations using the negative autoregressive parameter $\rho^{-} = -0{\cdot}9$ and positive autoregressive parameter $\rho^{+} = 0{\cdot}9$.

Fig. S5. The results of the floating grid permutation technique for analysing inbreeding avoidance in a simulated great tit population.

Fig. S6. The results of the floating grid permutation technique for size analysing assortative pairing in a freshwater shrimp (Example 2).

Fig. S7. The results of the floating grid permutation technique for analysing self-pollination in the gunsight clarkia (Example 3).

Fig. S8. Visiting counts of (a) the roe deer population without habitat selection and (b) the population with habitat selection at vegetation patches.

Fig. S9. Scatter plots of biomass versus visiting counts for the populations (a) without and (b) with habitat selection.

Fig. S10. The results of the floating grid permutation technique for analysing habitat selection in roe deer (Example 4).

Appendix S1 The floating grid permutation algorithm.